JRRD Volume 46, Number 3, 2009
Pages 361–374
Journal of Rehabilitation Research & Development

Agonist-antagonist active knee prosthesis: A preliminary study in level-ground walking

Ernesto C. Martinez-Villalpando, SM;[1] Hugh Herr, PhD[1–2*]
[1]Massachusetts Institute of Technology (MIT) Media Laboratory, Cambridge, MA; [2]Harvard-MIT Division of Health Sciences and Technology, Cambridge, MA

Abstract—We present a powered knee prosthesis with two series-elastic actuators positioned in parallel in an agonist-antagonist arrangement. To motivate the knee's design, we developed a prosthetic knee model that comprises a variable damper and two series-elastic clutch units that span the knee joint. Using human gait data to constrain the model's joint to move biologically, we varied model parameters using an optimization scheme that minimized the sum over time of the squared difference between the model's joint torque and biological knee values. We then used these optimized values to specify the mechanical and control design of the prosthesis for level-ground walking. We hypothesized that a variable-impedance control design could produce humanlike knee mechanics during steady-state level-ground walking. As a preliminary evaluation of this hypothesis, we compared the prosthetic knee mechanics of an amputee walking at a self-selected gait speed with those of a weight- and height-matched nonamputee. We found qualitative agreement between prosthetic and human knee mechanics. Because the knee's motors never perform positive work on the knee joint throughout the level-ground gait cycle, the knee's electrical power requirement is modest in walking (8 W), decreasing the size of the onboard battery required to power the prosthesis.

Clinical Trial Registration: ClinicalTrials.gov; Active Knee Prosthesis Study for Improvement of Locomotion for Above Knee Amputees, NCT00771589; http://clinicaltrials.gov/ct/show/NCT00771589.

Key words: agonist-antagonist actuation, biomimetic design, finite state machine, gait evaluation, human walking, impedance control, knee mechanics, knee prosthesis, rehabilitation, series-elastic actuation.

INTRODUCTION

Modern transfemoral prostheses can be classified into three major groups: passive, variable damping, and powered. Passive prosthetic knees do not require a power supply for their operation and are generally less adaptive to environmental disturbances than variable-damping prostheses. Variable-damping knees do require a power source but only to modulate damping levels, whereas powered prosthetic knees are capable of performing nonconservative positive knee work.

Variable-damping knees offer several advantages over mechanically passive designs, including enhanced knee stability and adaptation to different ambulatory speeds [1–6]. Examples of commercially available variable-damping knees include the Blatchford Endolite Intelligent Prosthesis, the Otto Bock C-Leg, and the Össur Rheo Knee. Although variable-damping knees offer some advantages over purely passive knee mechanisms, they are incapable of producing positive mechanical power and therefore cannot replicate the positive work phases of the human knee joint for such activities as sit-to-stand maneuvers, level-ground

Abbreviations: ES = early stance (phase), H = heel contact, HS = heel strike, MIT = Massachusetts Institute of Technology, PW = preswing (phase), SW = swing (phase), T = toe contact.

***Address all correspondence to Hugh Herr, PhD; Harvard-MIT Division of Health Sciences and Technology, 20 Ames St, Cambridge, MA 02139; 617-258-6574; fax: 617-253-8542. Email: hherr@media.mit.edu**

DOI:10.1682/JRRD.2008.09.0131

walking, and stair/slope ascent ambulation. Not surprisingly, transfemoral amputees experience clinical problems when using variable-damping knee technology. For example, amputees have asymmetric gait patterns, slower gait speeds, and elevated metabolic energy requirements than nonamputees [6].

Developing a commercially viable powered prosthesis that is humanlike in its weight, size, and strength, while still being energetically economical and noise free, is indeed a challenging design problem. Current approaches to the design of powered prostheses have focused mainly on the use of single-motor transmission systems directly coupled to the knee joint (http://www.ossur.com) [7–8]. Such direct-drive designs, however, require high electrical power consumption to fully emulate the mechanical behavior of the human knee joint, even during level-ground ambulation. One reason for this lack of energetic economy may be that such designs do not adequately leverage the passive dynamics of the leg and the elastic energy storage and return of tendonlike structures in a manner comparable to highly economical walking machine designs [9–11] or simpler mechanical knee designs with extension-assist compliant elements [12].

As a resolution to these difficulties, in this article we present the design and implementation of a knee prosthesis that comprises two series-elastic actuators positioned in parallel in an agonist-antagonist arrangement. To motivate the knee's design, we advanced a variable-impedance prosthetic knee model, comprising two series-elastic clutch mechanisms and a variable damper. Using human gait data to constrain the model's joint to move biologically, we varied model parameters with an optimization scheme that minimized the sum over time of the squared difference between the model's knee joint torque and biological knee values. We then used these optimized values to specify the mechanical and control design of the agonist-antagonist prosthesis. We hypothesized that a variable-impedance control design could produce humanlike knee mechanics during steady-state level-ground walking. As a preliminary evaluation of this hypothesis, we compared the prosthetic knee torque output of a unilateral transfemoral amputee walking at a self-selected gait speed with that of a weight- and height-matched nonamputee.

METHODS

In this section, we first review human knee biomechanics in walking. Using these biomechanical descriptions, we then define a variable-impedance prosthetic knee model that we use to motivate the agonist-antagonist prosthetic design. Finally, we describe the methods employed to assess the prosthesis's capacity to emulate human knee biomechanics.

Human Knee Biomechanics in Level-Ground Walking

Five distinct stages or gait phases have been used to describe knee biomechanics in level-ground walking (**Figure 1**). These gait phases are described as follows:

1. Beginning at heel strike (HS), the stance knee begins to flex slightly (~15°). This stance flexion phase allows for shock absorption upon impact. During this phase, the knee can be modeled as a spring (linear torque vs angle slope; **Figure 1(b)**), storing energy in preparation for the stance extension phase.
2. After maximum stance flexion is reached, the knee joint begins to extend (15% gait cycle) until maximum stance extension is reached (42% gait cycle). This knee extension period is called the stance extension phase. During stance extension, the knee acts as a spring (linear torque vs angle slope; **Figure 1(b)**), having similar stiffness* as during stance flexion.
3. During late stance or preswing (PW) (from 42% to 62% gait cycle), the knee of the supporting leg begins its rapid flexion period in preparation for the swing (SW) phase. During PW, as the knee begins to flex in preparation for toe-off, the knee acts as a spring (linear torque vs angle slope; **Figure 1(b)**), with a relatively lower stiffness than during stance flexion and extension.
4. As the hip is flexed, the leg leaves the ground and the knee continues to flex. At toe-off, the swing flexion phase of gait begins. Throughout this period (from 62% to 73% gait cycle), knee power is generally negative as the knee's torque impedes knee rotational velocity (**Figure 1(a)**). Thus, during swing flexion, the knee can be modeled as a variable damper.
5. After reaching a maximum flexion angle (~60°) during SW, the knee begins to extend forward. During swing extension (from 73% to 100% gait cycle), knee power is generally negative for deceleration of the swinging leg in preparation for the next stance period. Thus, as with swing flexion, during swing extension the knee can be modeled as a variable damper. After the knee

*Here stiffness is not actual joint stiffness by rather a quasi-static stiffness defined as the slope of the torque versus angle curve.

has reached full extension, the foot is once again placed on the ground and the next walking cycle begins.

Quasi-Passive Prosthetic Knee Model and Optimization

Given the knee biomechanics described in the last section, we anticipate that a variable-impedance knee prosthesis, capable of varying both damping and stiffness, can produce humanlike knee mechanics during steady-state level-ground walking. As a preliminary evaluation of this hypothesis and to motivate the prosthesis's design, we present a prosthetic knee model, shown in **Figure 2**, that comprises two antagonistic series-elastic clutches (to model the stance phase knee mechanics) and one

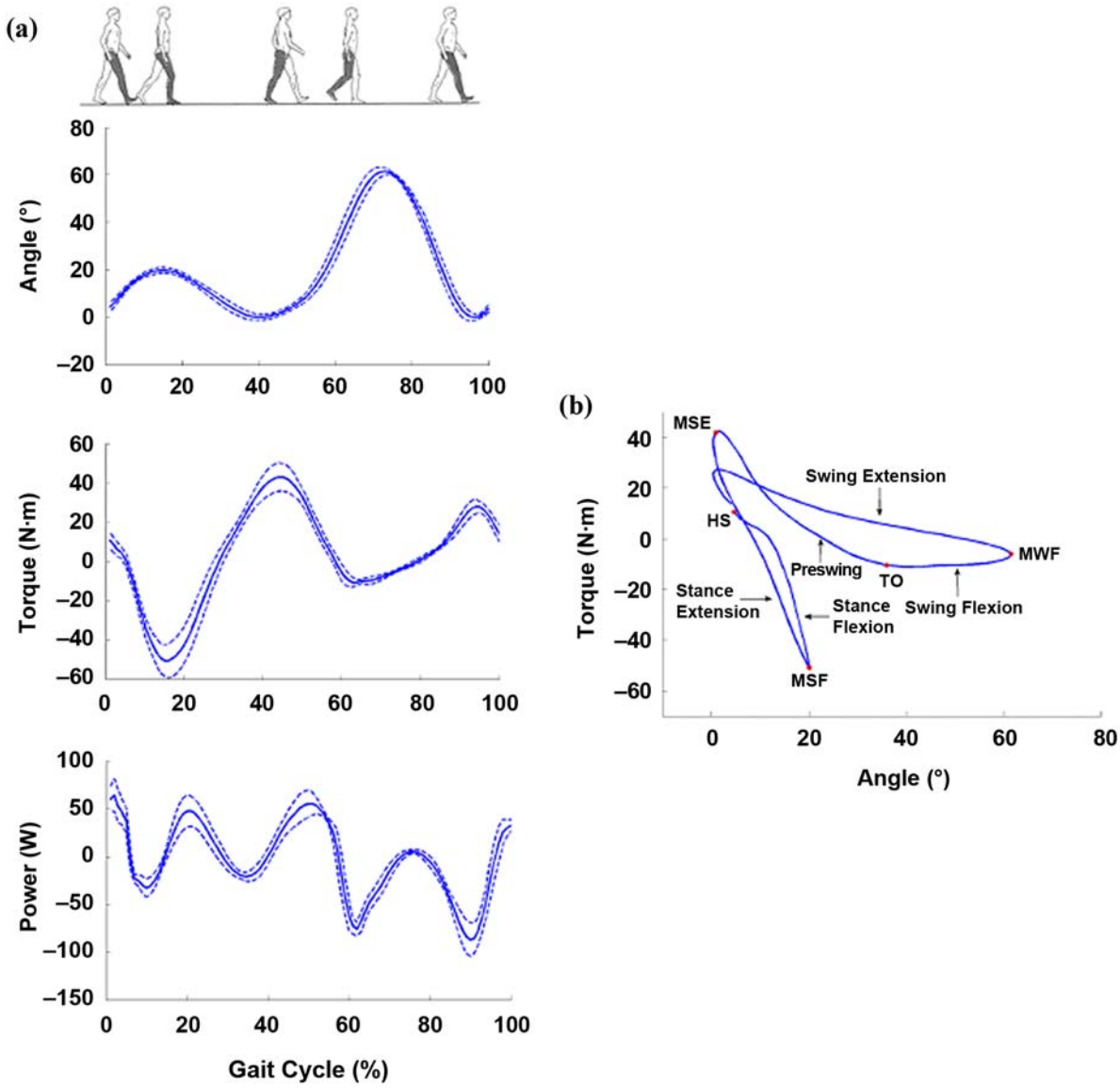

Figure 1.
Representative knee biomechanics in level-ground walking. **(a)** Knee angle, torque, and power curves of male study participant (mass = 81.9 kg) are plotted against percent gait cycle during level-ground walking at self-selected speed (1.31 m/s). Plotted are mean (solid line) ± 1 standard deviation (dashed lines) for $n = 10$ gait trials. **(b)** Knee torque is plotted versus knee angular position showing five phases of gait. Key gait events separating five phases are heel strike (HS), maximum stance flexion (MSF), maximum stance extension (MSE), toe-off (TO), and maximum swing flexion (MWF). Detailed description of how these gait data were collected and analyzed is presented in the "Methods—Intact-Limb Walking: Data Collection and Analysis" section (p. 365).

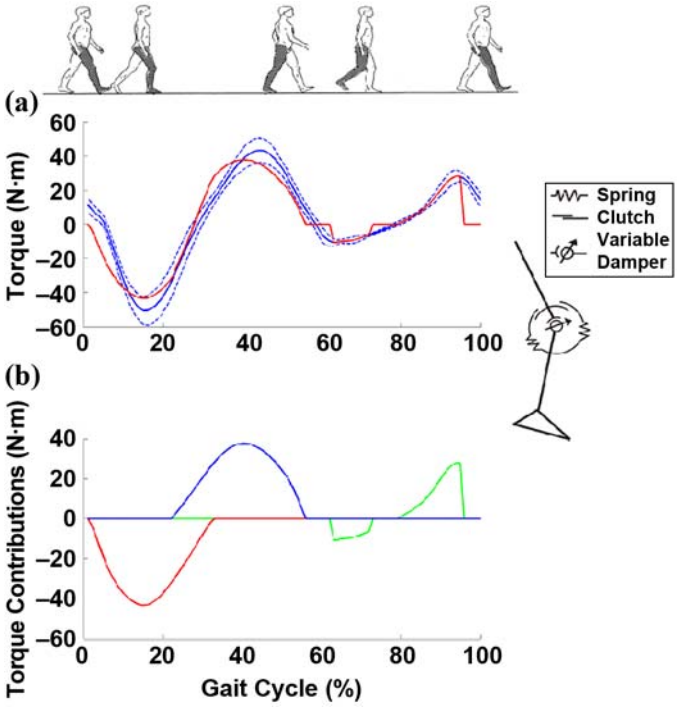

Figure 2.
Variable-impedance prosthetic knee model. Model, shown on right, comprises two monoarticular series-elastic clutches and one variable-damping element. **(a)** Optimized net torque output of knee model (red line) is compared with torque profile of intact human knee joint (mean [solid blue line] ± 1 standard deviation [dashed blue lines]; n = 10 gait trials). Biological data, adopted from **Figure 1**, are from study participant (mass = 81.9 kg) with intact limbs walking at self-selected speed (1.31 m/s). Detailed description of how these gait data were collected and analyzed is presented in the "Methods—Intact-Limb Walking: Data Collection and Analysis" section (p. 365). **(b)** Torque contributions from extension (red line) and flexion (blue line) springs of series-elastic clutch elements, as well as variable damper (green line). Optimizer gave extension spring stiffness equal to k_E = 160 N·m/rad, flexion spring stiffness equal to k_F = 137 N·m/rad, and knee engagement angle for flexion spring equal to 0.27 rad (15.46°). Extension spring was constrained to engage at instant of heel strike to ensure safety of amputee user.

variable-damping element (to model the SW phase mechanics). In the model, a series spring can be engaged by activating its respective clutch or disengaged by opening that clutch. As model constraints, each clutch can only be engaged once during each gait cycle. Additionally, once a clutch has been engaged, it only can be disengaged when the series spring has released all its energy and the force on the clutch is zero.

We varied series-elastic clutch model parameters, or two spring constants (k_E, k_F) corresponding to the extension* and flexion spring stiffness, and the relative knee extension and flexion angles (θ_E and θ_F), at which the extension and flexion springs become engaged during stance (knee angle convention is defined in the "Knee Control Design" section, p. 366).

The knee model was fitted to biomechanical data using an optimization scheme that minimized the sum over time of the squared difference between the model's knee joint torque and biological knee values. More specifically, the cost function used for the optimization was

$$E_{\text{cost}}(k_F,k_E,\theta_E,\theta_F) = \sum_{i=1}^{100}\left(\frac{\tau_{\text{bio}}^{i} \angle \tau_{\text{sim}}^{i}}{\tau^{\max}_{\text{bio}}}\right)^2, \qquad (1)$$

where τ_{bio}^{i} and τ_{sim}^{i} are the angular torques applied about the knee joint at the ith percentage of gait cycle from the biological torque data and the knee model, respectively, and $\tau^{\max}_{\text{bio}}$ is the maximum biological torque at the joint during the gait cycle. **Equation (1)** was minimized with the constraint that the extensor spring always engages at HS (θ_E = 0). We applied this constraint to limit knee buckling at HS as a safety measure for the amputee. We determined the desired global minimum for **Equation (1)** by first using a genetic algorithm to find the region containing the global minimum followed by an unconstrained gradient optimizer (fminunc in MATLAB® [The MathWorks, Inc; Natick, Massachusetts]) to determine the exact value of that global minimum. After optimizing **Equation (1)** by varying the parameters of the series-elastic clutch elements, we used the model's variable damper to achieve perfect agreement between the prosthetic knee model and biological torque values in regions where the series-elastic components were not able to absorb sufficient negative mechanical power.

The biological knee torque values were obtained from an inverse dynamics calculation using kinetic and kinematic data from 10 walking trials of a nondisabled 81.9 kg, 1.87 m tall subject walking at 1.31 m/s. A detailed description of how these kinetic and kinematic data were collected and analyzed is presented in the next section: "Intact-Limb Walking: Data Collection and Analysis."

*By convention, the extensor spring tends to extend the knee joint when engaged, whereas the flexor spring tends to cause the knee to flex.

Figure 2 shows the model optimization results plotted against the biological torque data from **Figure 1**. The model's torque output agrees well with experimental values. As constrained by the optimization procedure, the extension spring engages at HS, storing energy during early stance (ES) knee flexion. As the knee begins to extend, the flexion spring is engaged, storing energy as the extension spring releases its energy. During the SW phase, the model's variable damper exactly matches the biological torque values in regions of negative power. At mid- and terminal-SW phase, the power is positive in the biological data, and thus, the damper outputs zero torque in these gait regions.

Intact-Limb Walking: Data Collection and Analysis

Intact-limb kinetic and kinematic walking data were collected at the Gait Laboratory of Spaulding Rehabilitation Hospital, Harvard Medical School, in a study approved by the Spaulding Committee on the Use of Humans as Experimental Participants. One nondisabled, adult male volunteered for the study. The participant was asked to walk at a self-selected speed across a 10 m walkway in the Motion Analysis Laboratory for 10 consecutive trials. He was timed between two fixed points to ensure that the same walking speed was used between experimental trials. Walking speeds within a ±5 percent interval from the self-selected speed were accepted. The data collection procedures were based on standard techniques [13–17]. An infrared camera system (eight cameras, VICON 512 motion analysis system; Oxford Metrics, Oxford, United Kingdom) was used to measure the three-dimensional locations of reflective markers at 120 frames/s. A total of 33 markers was placed on various parts of a participant's body using the standard Plug-in Gait model: 16 lower-body markers, 5 trunk markers, 8 upper-limb markers, and 4 head markers. The markers were attached to the following bony landmarks: bilateral anterior superior iliac spines, posterior superior iliac spines, lateral femoral condyles, lateral malleoli, forefeet, and heels. Additional markers were rigidly attached to wands over the midfemur and midshaft of the tibia. The kinematics of the upper body were also collected with markers placed on the following locations: sternum; clavicle; seventh cervical vertebra; tenth thoracic vertebra; head; and bilaterally on the shoulder, elbow, and wrist. The VICON 512 system was able to detect marker position with a precision of ~1 mm.

During walking trials, ground reaction forces were measured synchronously with the kinematic data at a sampling rate of 1,080 Hz with two staggered force platforms (Advanced Mechanical Technology Inc; Watertown, Massachusetts) embedded in the walkway. The platforms measured ground reaction force and center of pressure location at a precision of ~0.1 N and ~2 mm, respectively. Prior to modeling and analysis, we used a fourth-order digital Butterworth filter at a cutoff frequency of 8 Hz to low-pass filter all marker position data. Filter frequency was based on the maximum frequency obtained from a residual analysis of all marker position data and processed as one whole gait cycle with 100 discrete data points from the HS to the next HS of the same leg. Joint torques and powers were then calculated using a standard inverse dynamics model (Vicon Bodybuilder, Oxford Metrics).

Knee Design

Electromechanics

Motivated by the prosthetic knee model described previously, we built an agonist-antagonist active knee prosthesis comprising two unidirectional, series-elastic actuators (**Figure 3**) [18–19]. Each unidirectional actuator of the knee prosthesis consists of a motor and a series spring connected via a transmission. The extension and flexion motors can be used independently to control the knee angle at which each series spring is engaged. As shown in **Figure 3**, the knee joint is rigidly coupled by a set of cables connected to a linear carriage that is free to move along the length of the device. This carriage can be engaged on either side by the extension and flexion springs, both of which are positioned by a ball screw driven by an electric motor. Both unidirectional series-elastic actuators feature transmissions comprised of a 2:1 belt drive coupled to a ball screw (10 × 3 mm, Nook Industries, Inc; Cleveland, Ohio). All actuation mechanisms are fully supported by an aluminum structure that resembles the lower-limb anatomical envelope. Each series-elastic actuator uses a brushed DC motor (Maxon RE40 and Maxon RE30 [Maxon Motor; Berkshire, United Kingdom], extension and flexion motors, respectively) capable of providing sufficient power for both level-ground walking and more energetically expensive tasks such as stair ascent.

A knee prosthesis should not exceed the size and weight of the missing limb and should exhibit similar

dynamics to those of a biological knee joint [20–21]. **Table 1** lists the design parameters for the active knee based on these functional requirements.

Sensors and Electronics

Feedback to the controller was provided by onboard intrinsic sensors (**Table 2**). In particular, locations and compressions for each series spring were monitored, as was the knee angular position. All electronics were implemented on a single board positioned along the lateral side of the knee. Motors were driven by H-bridge controllers with speed governed by 20 kHz pulse-width modulation and powered by a 6-cell Lithium polymer battery (22.2 V nominal). Analog sensors were read through a 10-bit analog-to-digital converter. The system was controlled by an AVR microcontroller and could be monitored by either USB or Bluetooth. Because all processing was done onboard and power was supplied by a relatively small battery (mass = 0.15 kg), the prototype was completely self-contained and did not require tethering.

Knee Control Design

A finite-state controller for level-ground walking was implemented to replicate the intact knee behavior shown in **Figure 1**. The three states of the controller were ES, PW, and SW. A quasi-passive equilibrium point control was implemented for ES and PW states, while variable-damping control was employed during the SW state. Transitions between states were determined primarily by three measurements: heel-ground contact, toe-ground contact, and knee angle. The finite-state control diagram

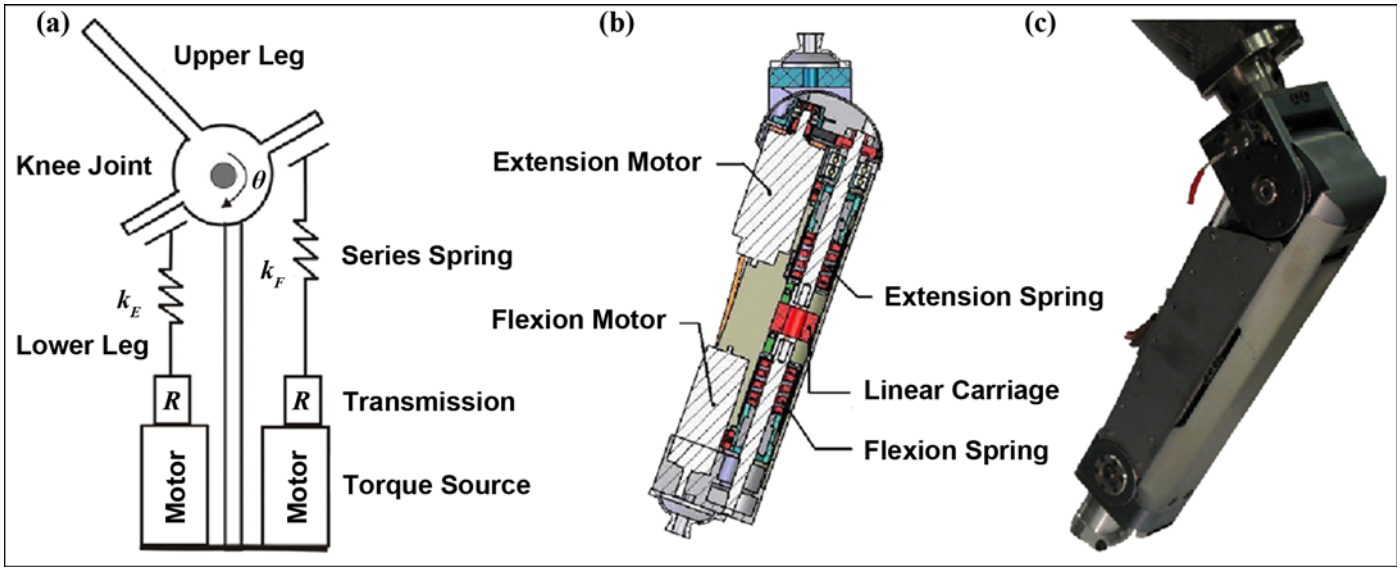

Figure 3.
Prosthesis design. **(a)** Simplified mechanical schematic of agonist-antagonist knee is shown. **(b)–(c)** Mechanical design and image of knee prosthesis, respectively. Flexion and extension spring rates for knee prosthesis were taken from knee model optimization results shown in **Figure 2**.

Table 1.
Knee size, angular range, and maximum torque values.

Variable	Value
Height	33 cm
Medio-Lateral Width	7 cm
Anterior-Posterior Width	7 cm
Total Weight	3 kg
Flexion Angle Range	0°–120°
Maximum Output Torque	130 N·m

Table 2.
Sensors used by prosthetic knee controller.

Measurement	Sensor
Ankle Angle	Digital encoder (linear)
Motor Displacements	Digital encoders (rotary)
Springs' Compression	Hall effect (ratiometric linear)
Heel/Toe Contact	Force sensitive resistor insole

indicating transitions is shown in **Figure 4**. For state transition and identification, the system relied on the following variables:

- Heel contact (H). H = 1 indicates that the heel is in contact with the ground, and H = 0 indicates the off-ground status.
- Toe contact (T). T = 1 indicates that the toe is in contact with the ground, and T = 0 indicates the off-ground status.
- Knee angle (θ) is the relative angle of the knee joint. All knee angles are flexion angles. Angles θ_E and θ_F define the angles at which the extension and flexion springs become engaged during stance, respectively. Further, θ_+ is the angle of the knee during swing flexion, and θ_- is the angle of the knee during swing extension.

Descriptions for each state are as follows:

1. ES begins at HS. When the heel contacts the ground (H = 1), the extension motor shaft is locked using a high proportional-derivative gain control with a desired shaft velocity equal to zero. The extension spring is then engaged with a spring equilibrium angle equal to the knee's position at HS θ_E. The extension spring then stores energy during ES knee flexion in preparation for knee extension. During knee flexion, the equilibrium point of the flexion spring θ_F is servoed via position control to closely track the linear carriage linked to the knee output joint. When the knee is maximally flexed in ES, the knee begins to extend and the flexion motor shaft is locked. The flexion spring then becomes engaged with a spring equilibrium angle equal to the knee's position at maximum knee flexion θ_F. Initially, energy is released from the extension spring and subsequently stored in the flexion spring.
2. PW begins as the heel leaves the ground (H = 0) and the knee angle becomes small (θ < 3°). In this state, the equilibrium point of the extension spring θ_F is position-controlled under zero load, tracking closely the linear carriage as the knee flexes in preparation for the SW phase. The flexion spring keeps holding its current equilibrium position θ_F (motor shaft locked). Thus, as the knee flexes throughout PW, the energy stored in the flexion spring is released.
3. SW begins at toe-off (T = 0). The extension spring equilibrium angle θ_E continues to track the knee angle under zero load. As the knee flexes beyond 20° (θ_+ > 20°) the flexion spring equilibrium angle θ_F is servoed under zero load to a position corresponding to θ = 15°. When the knee flexes past 60° (θ_+ > 60°), the extension spring is engaged. A low-gain damping control on the extension motor shaft causes the extension motor and transmission to back-drive, acting as a variable damper to reduce hyperflexion of the knee. Once the knee begins to extend and has an angle of less than 60° (θ_- < 60°), the extension spring equilibrium angle θ_E once again tracks the linear carriage under zero load to follow the knee throughout its extension. As the knee continues to extend past 15° in late swing, the flexion spring is engaged. Here again, a low-gain damping control on the flexion motor shaft causes the flexion motor and transmission to back-drive, acting as a variable damper to smoothly decelerate the swing leg until the flexion spring reaches an equilibrium angle θ_F of 3°. When the knee extends in swing beyond 5° (θ_- < 5°), the extension spring equilibrium angle θ_E is servoed to 3° in preparation for engagement and energy storage at HS of the subsequent gait cycle.

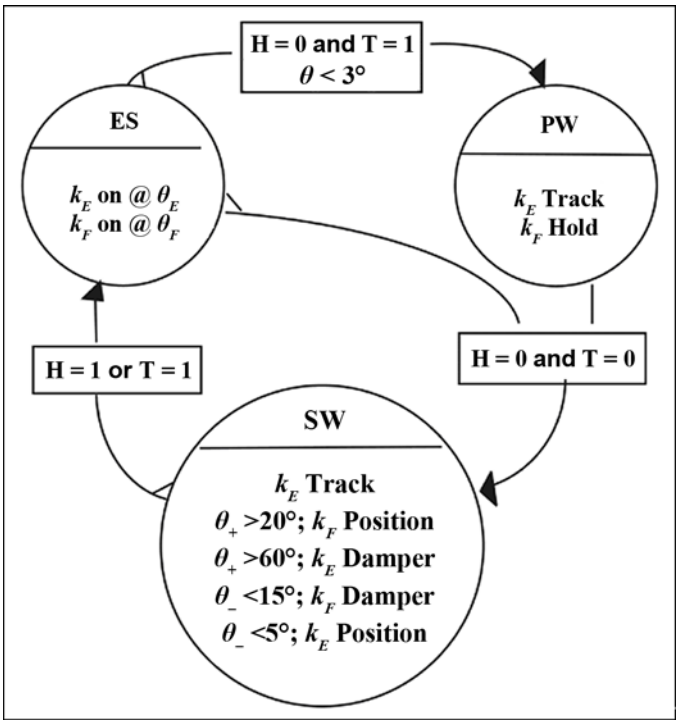

Figure 4.
Knee finite-state controller for level-ground walking. Three states are shown with control actions and transitional conditions. States are early stance (ES), preswing (PW), and swing (SW). H = heel contact, T = toe contact.

Amputee Walking: Data Collection and Analysis

We conducted a preliminary clinical study of the active knee prosthesis to evaluate the mechanical performance of the prosthesis using the finite-state machine controller. For this initial pilot investigation, we tested the device on a male unilateral amputee (mass = 97 kg, height = 1.86 m) who wore the powered knee prosthesis on his right leg attached to a conventional passive-elastic ankle-foot prosthesis (Flex-Foot LP-VariFlex® from Össur [Reykjavik, Iceland]).

Sensor readings and internal state were recorded from the device as the participant walked at self-selected speeds along a 10 m level-ground walkway. Parallel bars were available to the amputee for safety. A total of 10 walking trials was collected. Walking experiments were conducted in the Biomechatronics Research Group within the Massachusetts Institute of Technology (MIT) Media Laboratory and were approved by MIT's Committee on the Use of Humans as Experimental Subjects. The participant volunteered for the study and was permitted to withdraw from the study at any time and for any reason. Before taking part in the study, the participant read and signed a statement acknowledging informed consent.

RESULTS

In this section, we present the results obtained from the preliminary gait evaluation of the powered prosthesis during level-ground walking at a self-selected speed (0.81 m/s). The amputee participant and the prosthetist were satisfied with the performance of the prosthesis. In general, the participant took less than 20 minutes to adapt to and feel comfortable with the powered prosthesis.

The level-ground finite-state machine performed robustly throughout the experimental session. **Figure 5** shows data for three consecutive level-ground walking cycles. The control states for level-ground walking are defined as follows: ES = State 1, PW = State 2, and SW = State 3. The system went through the state sequence 1-2-3 (ES-PW-SW) for each walking cycle.

In **Figure 6**, prosthetic knee angle (**Figure 6(a)**), torque (**Figure 6(b)**), and power (**Figure 6(c)**) are plotted versus percent gait cycle. These prosthetic knee values show qualitative agreement with the intact knee mechanics shown in **Figure 1(a)** from a weight- and height-matched nonamputee. Similar to the knee kinematics of

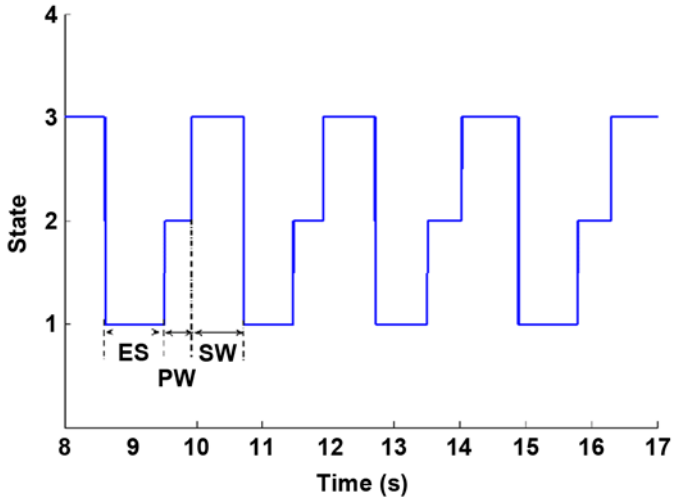

Figure 5.
Knee finite-state control transitions during amputee level-ground walking. Controller transitioned robustly from states 1-2-3 across 3 consecutive walking cycles. States are early stance (ES = State 1), preswing (PW = State 2), and swing (SW = State 3).

an intact knee, as shown in **Figure 6(a)**, the prosthetic knee exhibits ES knee flexion (peak flexion angle of ~14.5°) followed by knee extension. At terminal stance, the prosthetic knee undergoes rapid knee flexion in preparation for the SW phase. During the SW phase, the knee extends to a peak flexion angle of ~61° before extending forward prior to HS. As shown in **Figure 6(b)** and **(c)**, prosthetic knee torque and power are negative during ES knee flexion. For the intact knee data shown in **Figure 1(a)**, knee torque and power are initially positive following HS but quickly become negative as the knee continues to flex. The prosthetic knee exhibited similar behavior at the beginning of ES as shown in **Figure 6(b)**. This shift occurred because the amputee initially extended the knee right at HS, engaging the flexion spring, but quickly continued to flex the knee, engaging the extension spring. Compressing the extension spring immediately after HS helped protect the knee from excessive buckling so as to better ensure the amputee's safety. For both the intact and prosthetic knee, knee extension torque during stance is initially negative and then becomes positive and knee power is initially positive and then becomes negative. Further, during PW, torque and power are initially positive and then become negative in preparation for the SW phase. During SW, for both intact and prosthetic knees, power is generally negative to limit peak knee flexion (negative

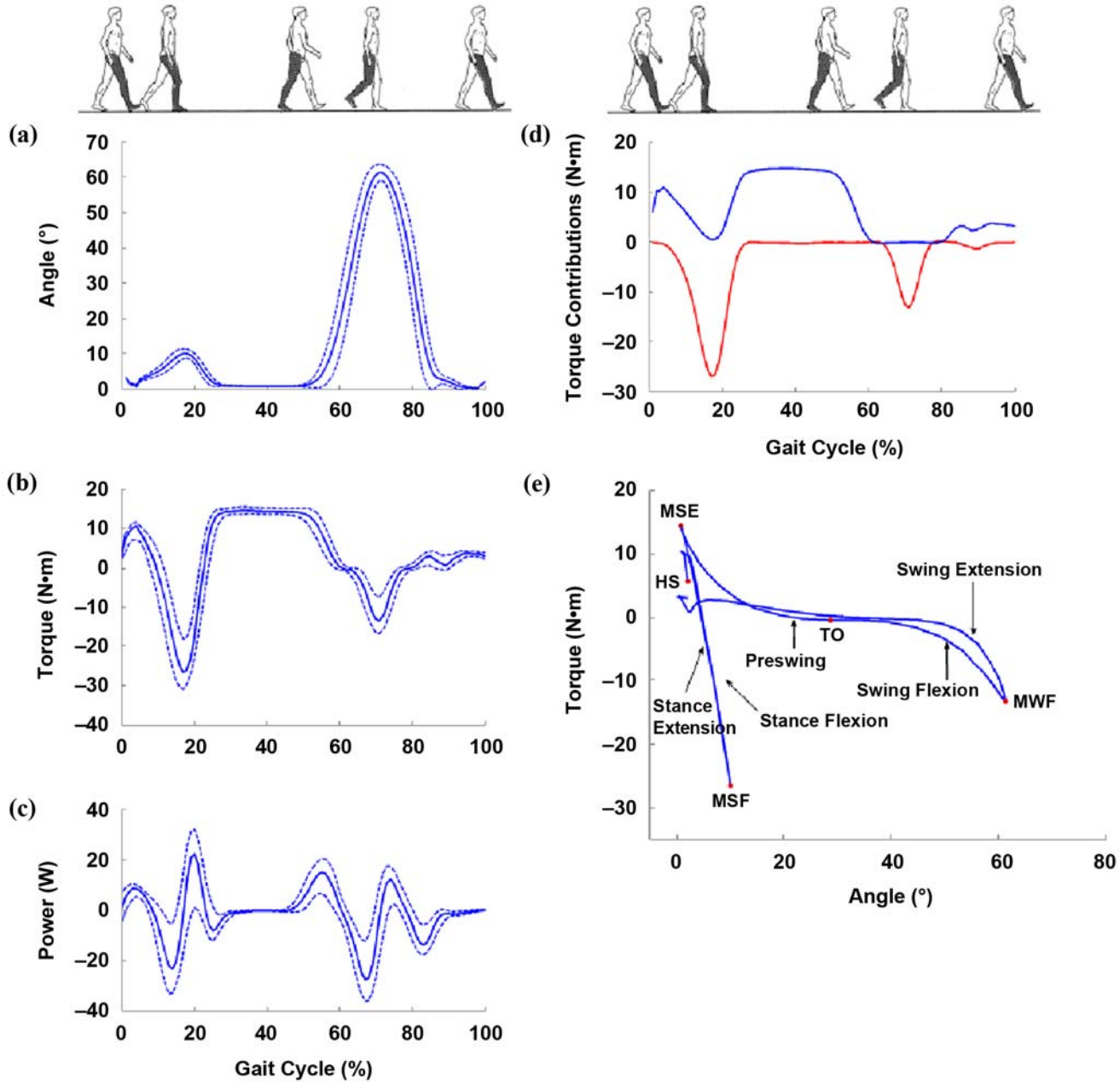

Figure 6.
Prosthetic knee mechanics. **(a)** Prosthetic knee angle, **(b)** net torque, and **(c)** power are plotted versus percent gait cycle (mean [solid blue line] ± 1 standard deviation [dashed blue lines]; *n* = 10 gait trials) for level-ground walking (amputee participant mass = 97 kg; walking speed = 0.81 m/s). **(d)** Torque contributions from extension (red line) and flexion (blue line) springs of series-elastic actuators are plotted. **(e)** Knee torque is plotted versus knee angular position, showing two characteristic stiffnesses during stance. HS = heel strike, MSE = maximum stance extension, MSF = maximum stance flexion, MWF = maximum swing flexion, TO = toe-off.

torque) and then to smoothly decelerate the swinging leg during swing extension (positive torque).

The torque contributions from each unidirectional series-elastic actuator versus percent gait cycle are plotted in **Figure 6(d)**. We observe the flexion spring is briefly engaged right after HS because of the amputee's short knee extension. At the instant stance knee flexion occurs, the extension spring is engaged, similar to the

prosthetic knee model. During stance flexion, the flexion spring loses its energy quickly as it closely tracks the linear carriage linked to the knee output joint. Subsequently, the flexion spring is engaged again at peak knee flexion during ES and stores energy during stance extension and PW. In SW, the extension motor at peak knee flexion and the flexion motor at terminal stance are actively backdriven to limit peak knee flexion and to smoothly decelerate the swinging leg at terminal stance, respectively.

In **Figure 6(e)**, prosthetic knee torque is plotted versus knee angular position. Like the intact human knee (**Figure 1(b)**), the prosthesis has two characteristic stiffnesses during stance. During ES flexion and extension phases, knee stiffness is relatively greater than during PW.

DISCUSSION

In this investigation, we sought to advance a viable powered knee prosthesis that is humanlike in its weight, size, and dynamics while still being energetically economical for level-ground walking. Current approaches to the design of powered prostheses have focused mainly on the use of single-motor transmission systems directly coupled to the knee joint (http://www.ossur.com) [7–8]. Such direct-drive designs, however, require a high electrical power consumption (>25 W) to fully emulate the mechanical behavior of the human knee joint even during level-ground ambulation. Possible causes for such high electrical power requirements are that such designs do not adequately leverage the passive dynamics of the leg [9–10] and elastic energy storage and return of tendon-like structures [11], both of which are key strategies that result in the relatively high metabolic walking economy of humans.

In this article, we presented the design and implementation of a knee prosthesis that comprises two unidirectional series-elastic actuators positioned in parallel in an agonist-antagonist arrangement. Because of its architecture, the knee can be controlled to behave as agonist-antagonist series-elastic clutch elements during the stance phase and as a variable-damper during the SW phase (see knee model in **Figure 2**), resulting in an energetically economical knee prosthesis for level-ground walking. Using such a variable-impedance knee control, we demonstrated qualitative agreement between prosthetic and intact knee mechanics during level-ground ambulation (**Figures 1** and **6**).

It is important to note that since the knee design is fully motorized with series-elastic force sensing, knee joint torque can be directly controlled for more energetically expensive tasks, such as stair and ramp ascent, as well as standing from a seated posture. Hence, the knee architecture is designed to accommodate nonconservative high mechanical-power movements while still providing for a highly economical level-ground walking mode, as demonstrated in this study.

Because of the variable-impedance prosthetic control during level-ground walking, the electrical power requirements* were low (8 W electrical) during steady-state walking trials at a speed of 0.81 m/s. Using step-count monitoring systems, researchers have determined that active unilateral amputees walk 3,060 ± 1,890 steps per day [22]. Assuming the case of an amputee walking for 5,000 steps at a moderate walking speed, how large would the onboard battery have to be? Using a lithium-polymer battery (energy density 165 W-h/kg [e.g., http://www.thunderpowerrc.com]), a 0.13 kg battery would enable 5,000 steps of powered walking (8 W × 1.95 s/cycle × 5000 cycles = 78 kJ). This battery mass is more than fivefold smaller than the required battery for Össur's Power Knee that is now being sold commercially.

Prosthetic Knee Design for Variable-Speed Walking

The active prosthetic knee proposed here is intended for amputees who have the ability to ambulate at a Medicare Functional Classification K3 level (i.e., having the ability or potential for ambulation with variable cadence). Does the variable-impedance model shown in **Figure 2** allow for adaptation to variable gait from slow to fast walking speeds? To evaluate this question, we fitted the variable-impedance knee model to biomechanical data from an intact subject walking at 1.0 m/s, 1.3 m/s, and 1.6 m/s using the optimization scheme described in the "Quasi-Passive Prosthetic Knee Model and Optimization" section (p. 363). The optimization results provided linear stiffness values (at each walking speed) for both series-elastic components, including their engagement angles during the walking cycle. For each spring and walking speed, we first selected the maximum force-displacement

*To estimate motor electrical power requirements (power = current × voltage), we used onboard motor current sensing to directly measure the current of each motor, and to estimate motor voltages, we used motor speeds, motor speed constants, and motor resistances.

data pairs. By plotting all data pairs in the same force versus displacement space, we were able to estimate the optimal nonlinear spring functions for the flexion and extension springs. **Figure 7(b)** shows the results of the nonlinear fit for both series-elastic elements. In particular, we implemented a second-order polynomial fit for the extension spring and a piecewise polynomial fit for the flexion spring. Both fits were implemented using the MATLAB® curve-fitting toolbox. Using these nonlinear spring functions, we then compared the prosthetic knee model output torque with the biological knee torque data. **Figure 7(c)** through **7(e)** shows this comparison for the three different walking speeds using the model shown in **Figure 7(a)**.

From **Figure 7(b),** we observe that the model's series-elastic elements describe a nonlinear stiffness behavior. These results suggest that in order to have a prosthetic knee that can adapt to amputee speed variations and still maintain an optimal level of energetic economy, both series springs have to be nonlinear and adjusted to the amputee's weight. The extension series-elastic component has to be replaced by a nonlinear hardening spring and the flexion component by a softening spring. Currently, the prosthetic knee employed in this study takes advantage of the implemented variable-impedance controller for minimum energy consumption but only for moderate walking speeds. In future hardware implementations, nonlinear springs will be employed for the knee's series-elastic elements so as to

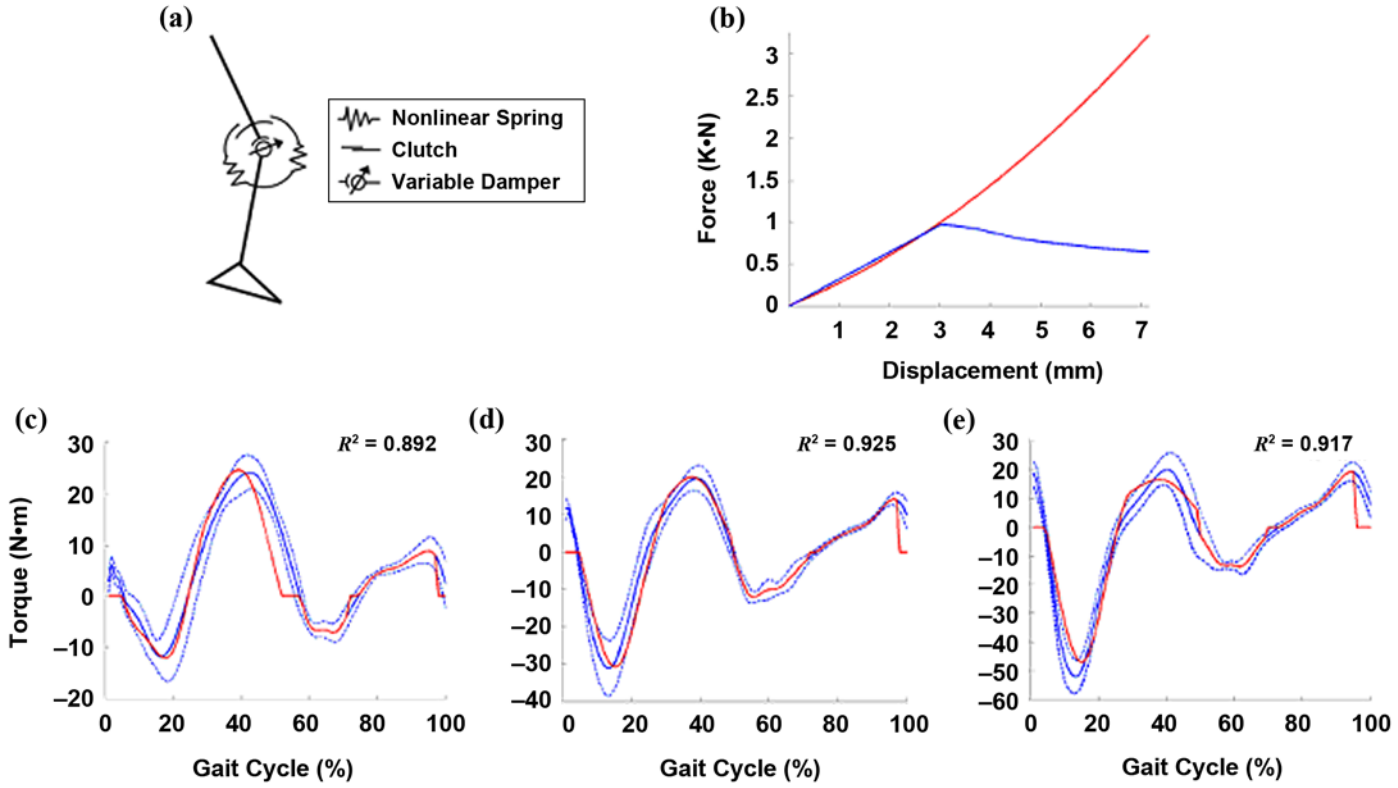

Figure 7.
Variable-impedance prosthetic knee model for variable-speed walking. **(a)** Model comprises two monoarticular series-elastic clutches and variable-damping element. **(b)** Optimized nonlinear polynomial fits are shown for force versus displacement behavior of model's extension spring (in red) and flexion spring (in blue). **(c)–(e)** Net torque output of optimized knee model (red line) is compared with torque profile of intact human knee joint (mean [solid blue lines] ± 1 standard deviation [dashed blue lines]; n = 10 gait trials). Goodness of fit for model is provided by coefficient of determination R^2 at each walking speed. Biological data are from study participant (mass = 66.2 kg) with intact limbs walking at three different speeds: **(c)** 1.0 m/s, **(d)** 1.3 m/s, and **(e)** 1.6 m/s. Walking speeds within ±5% for each selected speed were accepted. Intact gait data were collected at the Massachusetts Institute of Technology (MIT) gait and motion capture laboratory and analyzed using the same methodology as described in the section "Intact-Limb Walking: Data Collection and Analysis" (p. 365). Study was approved by MIT's Committee on the Use of Humans as Experimental Subjects.

achieve both speed adaptiveness and optimal energetic economy.

Clinical Relevance

In this investigation, we observed biomechanical improvements in the participant's gait with the active knee prosthesis. In addition to an evident ES knee flexion, we observed two positive power output bursts at midstance and late stance that are qualitatively comparable to intact knee behavior (**Figure 6**). In addition to the novel mechanical architecture, the variable-impedance control implemented in the knee allows for adaptation to the different phases of gait and walking speed, while maintaining a minimal electrical energy cost. We anticipate that this active knee will offer an improved metabolic economy of gait compared with variable-damping and mechanically passive prostheses in addition to a decrease in positive work generation at the hip during terminal stance and PW. In future clinical work, we plan to conduct a comprehensive gait study involving more amputee participants and including the measurement of metabolic, electromyographic, kinematic, and kinetic gait data. Such an investigation will provide a quantitative understanding of the effects of biomimetic knee prostheses on amputee locomotion.

CONCLUSIONS

A computationally and energetically autonomous knee prosthesis with unidirectional agonist-antagonist series-elastic actuators was presented. The knee employs series-elastic components optimized to minimize the electrical energy cost of level-ground walking. Using a variable-impedance control design, we demonstrated qualitative agreement between prosthesis and intact knee mechanics. The knee's motors did not perform positive work on the knee joint during level-ground walking trials, resulting in a modest electrical power requirement (8 W).

Future work with this prosthetic design will include the incorporation of a muscle-skeletal reflex controller to improve system adaptiveness to terrain variations. This controller will allow for better antistumble stance control and improved custom adaptation to individual gait. We hope that this work will motivate additional studies focused on the advancement of multifunctional lower-limb prostheses.

ACKNOWLEDGMENTS

Author Contributions:

Study concept and design: E. C. Martinez-Villalpando, H. Herr.

Study supervision: H. Herr.

Acquisition, analysis, and interpretation of data: E. C. Martinez-Villalpando, H. Herr.

Drafting of manuscript: E. C. Martinez-Villalpando, H. Herr.

Critical revision of manuscript: H. Herr.

Financial Disclosures: The authors have declared that no competing interests exist.

Funding/Support: This material was based on work supported by the Department of Veterans Affairs, grant VA241-P-0026.

Additional Contributions: We would like to acknowledge the contributions of MIT researchers Jeff Weber and Grant Elliott for their invaluable electromechanical design work.

Participant Follow-up: The authors plan to inform participants of the publication of this study.

REFERENCES

1. Flowers WC. A man-interactive simulator system for above-knee prosthetics studies [thesis]. Cambridge (MA): Department of Mechanical Engineering, Massachusetts of Institute Technology; 1972.
2. James K, Stein RB, Rolf R, Tepavic D. Active suspension above-knee prosthesis. In: Goh JCH, Nathan A, editors. Proceedings of the 6th International Conference on Biomedical Engineering; 1990 Dec 6–8; Singapore; 1990. p. 317–20.
3. Kitayama I, Nakagawa N, Amemori K. A microcomputer controlled intelligent A/K prosthesis. In: Proceedings of the 7th World Congress of the International Society for Prosthetics and Orthotics; 1992 Jun 28–Jul 3; Chicago, IL. Alexandria (VA): International Society for Prosthetics and Orthotics; 1992.
4. Zahedi S. The results of the field trial of the Endolite Intelligent Prosthesis. In: Proceedings of the 12th International Congress of INTERBOR; 1993 Sep 22–25; Lisbon, Portugal. Dublin (OH): International Society for Prosthetics and Orthotics; 1993.
5. Herr H, Wilkenfeld A. User-adaptive control of a magnetorheological prosthetic knee. Ind Rob. 2003;30(1):42–55. DOI:10.1108/01439910310457706
6. Johansson JL, Sherrill DM, Riley PO, Bonato P, Herr H. A clinical comparison of variable-damping and mechanically passive prosthetic knee devices. Am J Phys Med Rehabil. 2005;84(8):563–75. [PMID: 16034225] DOI:10.1097/01.phm.0000174665.74933.0b
7. Kapti AO, Yucenur MS. Design and control of an active artificial knee joint. Mech Mach Theory. 2006;41(12): 1477–85. DOI:10.1016/j.mechmachtheory.2006.01.017

8. Fite K, Mitchell J, Sup F, Goldfarb M. Design and control of an electrically powered knee prosthesis. In: Proceedings of the IEEE 10th International Conference on Rehabilitation Robotics; 2007 Jun 13–15; Noordwijk, the Netherlands. Piscataway (NJ): IEEE; 2007. p. 902–5.
9. McGeer T. Passive dynamic walking. Int J Robot Res. 1990;9(2):62–68. DOI:10.1177/027836499000900206
10. Wisse M. Essentials of dynamic walking: Analysis and design of two-legged robots [thesis]. Delft (the Netherlands): Technical University of Delft; 2004.
11. Endo K, Paluska D, Herr H. A quasi-passive model of human leg function in level-ground walking. In: Proceedings of the IEEE/RSJ International Conference on Intelligent Robots and Systems; 2006 Oct 9–16; Beijing, China. Piscataway (NJ): IEEE; 2006. p. 4935–39.
12. Radcliffe CW. The Knud Jansen Lecture: Above-knee prosthetics. Prosthet Orthot Int. 1977;1(3):146–60. [PMID: 617371]
13. Kadaba MP, Ramakrishnan HK, Wootten ME, Gainey J, Gorton G, Cochran GV. Repeatability of kinematic, kinetic, and electromyographic data in normal adult gait. J Orthop Res. 1989;7(6):849–60. [PMID: 2795325] DOI:10.1002/jor.1100070611
14. Kadaba MP, Ramakrishnan HK, Wootten ME. Measurement of lower extremity kinematics during level walking. J Orthop Res. 1990;8(3):383–92. [PMID: 2324857] DOI:10.1002/jor.1100080310
15. Winter DA. Biomechanics and motor control of human movement. 2nd ed. New York (NY): Wiley; 1990.
16. Kerrigan DC, Della Croce U, Marciello M, Riley PO. A refined view of the determinants of gait: Significance of heel rise. Arch Phys Med Rehabil. 2000;81(8):1077–80. [PMID: 10943758] DOI:10.1053/apmr.2000.6306
17. Kerrigan DC, Riley PO, Lelas JL, Della Croce U. Quantification of pelvic rotation as a determinant of gait. Arch Phys Med Rehabil 2001;82(2):217–20. [PMID: 11239313] DOI:10.1053/apmr.2001.18063
18. Pratt GA, Williamson MM. Series elastic actuators. In: Proceedings of Intelligent Robots and Systems 95: Human Robot Interaction and Cooperative Robots, IEEE/RSJ International Conference, Vol. 1; 1995 Aug 5–9; Pittsburgh, PA. Piscataway (NJ): IEEE; 1995. p. 399–406.
19. Robinson DW, Pratt JE, Paluska DJ, Pratt GA. Series elastic actuator development for a biomimetic walking robot. In: Proceedings of the IEEE/ASME International Conference on Advanced Intelligent Mechatronics; 1999 Sep 19–23; Atlanta, GA. Piscataway (NJ): IEEE; 1999. p. 561–68.
20. Winter DA, Robertson DG. Joint torque and energy patterns in normal gait. Biol Cybern. 1978;29(3):137–42. [PMID: 667202] DOI:10.1007/BF00337349
21. Braune W, Fischer O. Determination of the moments of inertia of the human body and its limbs. Berlin (Germany): Springer-Verlag; 1988.
22. Stepien JM, Cavenett S, Taylor L, Crotty M. Activity levels among lower-limb amputees: Self-report versus step activity monitor. Arch Phys Med Rehabil. 2007;88(7):896–900. [PMID: 17601471] DOI:10.1016/j.apmr.2007.03.016

Submitted for publication October 14, 2008. Accepted in revised form May 19, 2009.